Varieties of Dynamic Multiscaling in Fluid Turbulence

Dhrubaditya Mitra and Rahul Pandit*

Centre for Condensed Matter Theory, Department of Physics, Indian Institute of Science, Bangalore 560012, India

(Received 10 September 2003; published 6 July 2004)

We show that different ways of extracting time scales from time-dependent velocity structure functions lead to different dynamic-multiscaling exponents in fluid turbulence. These exponents are related to equal-time multiscaling exponents by different classes of bridge relations, which we derive. We check this explicitly by detailed numerical simulations of the Gledzer-Ohkitani-Yamada shell model for fluid turbulence. Our results can be generalized to any system in which both equal-time and time-dependent structure functions show multiscaling.

DOI: 10.1103/PhysRevLett.93.024501 PACS numbers: 47.27.Gs, 47.27.Eq

The dynamic scaling of time-dependent correlation functions in the vicinity of a critical point was understood soon after the scaling of equal-time correlations [1]. The development of a similar understanding of the dynamic multiscaling of time-dependent velocity structure functions in homogeneous, isotropic fluid turbulence should have implications for the temporal intermittency of eddies advected by the mean flow. But studies of such dynamic multiscaling still lag far behind their analogs for the multiscaling of equal-time velocity structure functions [2]. There are three major reasons for this: (i) The multiscaling of equal-time velocity structure functions in fluid turbulence [2] is far more complex than the scaling of equal-time correlation functions in critical phenomena. (ii) The dynamic scaling of Eulerian-velocity structure functions is dominated by sweeping effects that relate temporal and spatial scales linearly and thus lead to a trivial dynamic-scaling exponent $z_{\mathcal{E}} = 1$, where the subscript $\mathcal{E}$ stands for Eulerian. (iii) Even if this dominant temporal scaling because of sweeping effects is removed (see below), time-dependent velocity structure functions do not have simple scaling forms (Ref. [3]) and an infinity of dynamic-multiscaling exponents is required. The dynamic-multiscaling exponents are related to the equal-time multiscaling exponents by bridge relations, one class of which were obtained in Ref. [3]. In the forced-Burgers-turbulence context, a few bridge relations of another class were obtained in Refs. [4,5]. If the bridge relations of Refs. [3–5] are compared naively, then they disagree with each other. However, the crucial point about dynamic multiscaling, not enunciated clearly hitherto, although partially implicit in Refs. [3–5], is that different ways of extracting time scales from time-dependent velocity structure functions yield different dynamic-multiscaling exponents that are related to the equal-time multiscaling exponents by different classes of bridge relations. We systematize such bridge relations by distinguishing three types of methods that can be used to extract time scales; these are based, respectively, on integral I, derivative D, and exit-time E scales. We derive the bridge relations for dynamic-multiscaling exponents for these three methods and check by an extensive numerical simulation that such bridge relations hold in the Gledzer-Ohkitani-Yamada (GOY) shell model for fluid turbulence.

To proceed further, let us recall that in homogeneous, isotropic turbulence, the equal-time, order-p, velocity structure function $S_p(\ell) \equiv \langle [\delta v_\parallel(\vec{x}, t, \ell)]^p \rangle \sim \ell^{\zeta_p}$, for $\eta_d \ll \ell \ll L$, where $\delta v_\parallel(\vec{x}, t, \ell) = [\vec{v}(\vec{x} + \vec{\ell}, t) - \vec{v}(\vec{x}, t)] \times (\vec{\ell}/\ell)$, $\vec{v}(\vec{x}, t)$ is the fluid velocity at point $\vec{x}$ and time t, L is the large spatial scale at which energy is injected into the system, η_d is the small length scale at which viscous dissipation becomes significant, ζ_p is the order-p, equal-time multiscaling exponent, and the angular brackets denote an average over the statistical steady state of the turbulent fluid. The 1941 theory (K41) of Kolmogorov [6] yields the simple scaling result $\zeta_p^{\mathrm{K41}} = p/3$. However, experiments and simulations indicate multiscaling; i.e., ζ_p is a nonlinear, convex function of p; and the von Kármán–Howarth relation [2] yields $\zeta_3 = 1$. To study dynamic multiscaling we use the longitudinal, time-dependent, order-p structure function [3]

$$\mathcal{F}_p(\ell, \{t_1, \ldots, t_p\}) \equiv \langle [\delta v_\parallel(\vec{x}, t_1, \ell) \ldots \delta v_\parallel(\vec{x}, t_p, \ell)] \rangle. \quad (1)$$

Clearly, $\mathcal{F}_p(\ell, \{t_1 = \ldots = t_p = 0\}) = S_p(\ell)$. We normally restrict ourselves to the simple case $t_1 = t_2 = \ldots = t_q \equiv t$ and $t_{q+1} = t_{q+2} = \ldots = t_p = 0$, for notational simplicity write $\mathcal{F}_p(\ell, t)$, and suppress the q dependence which should not affect dynamic-multiscaling exponents (see below). To remove the sweeping effects mentioned above, we must of course use quasi-Lagrangian [3,7] or Lagrangian [8] velocities in Eq. (1), but we do not show this explicitly here for notational convenience. Given $\mathcal{F}_p(\ell, t)$, we can extract a characteristic time scale $\tau_p(\ell)$ in several different ways, as we describe later. The dynamic-multiscaling ansatz $\tau_p(\ell) \sim \ell^{z_p}$ can now be used to determine the order-p dynamic-multiscaling exponents z_p. Furthermore, a naive extension of K41 to dynamic scaling [9] yields $z_p^{\mathrm{K41}} = \zeta_2^{\mathrm{K41}} = 2/3$ for all p.

In the multifractal model [2] the velocity of a turbulent flow is assumed to possess a range of universal scaling

exponents $h \in I \equiv (h_{\min}, h_{\max})$. For each h in this range, there exists a set $\Sigma_h \subset \mathbb{R}^3$ of fractal dimension $D(h)$, such that $\delta v(\vec{r}, \ell)/v_L \propto (\ell/L)^h$ for $\vec{r} \in \Sigma_h$, with v_L the velocity at the forcing scale L, whence

$$\frac{S_p(\ell)}{v_L^p} \equiv \frac{\langle \delta v^p(\ell) \rangle}{v_L^p} \propto \int_I d\mu(h) \left(\frac{\ell}{L}\right)^{\mathcal{Z}(h)}, \tag{2}$$

where $\mathcal{Z}(h) = [ph + 3 - D(h)]$, the measure $d\mu(h)$ gives the weight of the fractal sets, and a saddle-point evaluation of the integral yields $\zeta_p = \inf_h[\mathcal{Z}(h)]$. The ph term in $\mathcal{Z}(h)$ comes from p factors of (ℓ/L) in Eq. (2); the $3 - D(h)$ term comes from an additional factor of $(\ell/L)^{3-D(h)}$, which is the probability of being within a distance $\sim \ell$ of the set Σ_h of dimension $D(h)$ that is embedded in three dimensions. Similarly, for the time-dependent structure function

$$\frac{\mathcal{F}_p(\ell, t)}{v_L^p} \propto \int_I d\mu(h) \left(\frac{\ell}{L}\right)^{\mathcal{Z}(h)} \mathcal{G}^{p,h}\left(\frac{t}{\tau_{p,h}}\right), \tag{3}$$

where $\mathcal{G}^{p,h}(t/\tau_{p,h})$ has a characteristic decay time $\tau_{p,h} \sim \ell/\delta v(\ell) \sim \ell^{1-h}$, and $\mathcal{G}^{p,h}(0) = 1$. If $\int_0^\infty t^{(M-1)} \mathcal{G}^{p,h} dt$ exists, we can define the order-p, degree-M, integral time scale

$$\mathcal{T}^{\,I}_{p,M}(\ell) \equiv \left[\frac{1}{S_p(\ell)} \int_0^\infty \mathcal{F}_p(\ell, t) t^{(M-1)} dt\right]^{(1/M)}. \tag{4}$$

We can now define the integral dynamic-multiscaling exponents $z^I_{p,M}$ via $\mathcal{T}^{\,I}_{p,M} \sim \ell^{z^I_{p,M}}$. By substituting the multifractal form (3) in Eq. (4), computing the time integral first, and then performing the integration over the multifractal measure by the saddle-point method, we obtain the integral bridge relation

$$z^I_{p,M} = 1 + [\zeta_{p-M} - \zeta_p]/M, \tag{5}$$

which was first obtained in Ref. [3]. Likewise, if $(\partial^M/\partial t^M)\mathcal{G}^{p,h}|_{t=0}$ exists, we can define the order-p, degree-M, derivative time scale

$$\mathcal{T}^{\,D}_{p,M} \equiv \left[\frac{1}{S_p(\ell)} \frac{\partial^M}{\partial t^M} \mathcal{F}_p(\ell, t)|_{t=0}\right]^{(-1/M)}, \tag{6}$$

the derivative dynamic-multiscaling exponents $z^D_{p,M}$ via $\mathcal{T}^{\,D}_{p,M} \sim \ell^{z^D_{p,M}}$, and thence obtain the derivative bridge relation

$$z^D_{p,M} = 1 + [\zeta_p - \zeta_{p+M}]/M. \tag{7}$$

Such derivative bridge relations, for the special cases (a) $p = 2, M = 1$ and (b) $p = 2, M = 2$, were first obtained in the forced-Burgers-turbulence context in Refs. [5] and [4], respectively, without using quasi-Lagrangian velocities but by using other methods to suppress sweeping effects [10]. Case (a) yields the interesting result $z^D_{2,1} = \zeta_2$, since $\zeta_3 = 1$. Both relations (5) and (7) reduce to $z_p^{\mathrm{K41}} = 2/3$ if we assume K41 scaling for the equal-time structure functions.

If we consider n nonzero time arguments for the structure function $\mathcal{F}_{p,n}(\ell, t_1, \ldots, t_n, \ldots, 0 \ldots, 0)$, which we denote by $\mathcal{F}_{p,n}(\ell, t_1, \ldots, t_n)$ for notational simplicity, we can define the integral-time scale, $\mathcal{T}^{\,I}_{p,M,n}(\ell) \equiv [1/S_p(\ell) \int_0^\infty \mathcal{F}_p(\ell, t_1, \ldots, t_n) t_1^{m_1 - 1} dt_1 \ldots t_n^{m_n - 1} dt_n]^{1/(Mn)}$, and the derivative-time scale, $\mathcal{T}^{\,D}_{p,M,n}(\ell) \equiv [1/S_p(\ell) \times (\partial^{m_1}/\partial t_1^{m_1}) \cdots (\partial^{m_n}/\partial t_n^{m_n}) \mathcal{F}_p(\ell, t_1, \ldots, t_n)|_{t_1 = 0, \ldots, t_n = 0}]^{-1/(Mn)}$, where $M = \sum_{i=1}^n m_i$. From these we can obtain, as above, two generalized bridge relations:

$$\begin{aligned} z^I_{p,M,n} &= 1 + (\zeta_{p-nM} - \zeta_p)/(nM); \\ z^D_{p,M,n} &= 1 + (\zeta_p - \zeta_{p+nM})/(nM). \end{aligned} \tag{8}$$

We now study time-dependent structure functions of the GOY shell model for fluid turbulence [2,11,12]:

$$\left(\frac{d}{dt} + \nu k_n^2\right) u_n = i(a_n u_{n+1} u_{n+2} + b_n u_{n-1} u_{n+1} + c_n u_{n-1} u_{n-2})^* + f_n. \tag{9}$$

Here the complex, scalar velocity u_n, for the shell n, depends on the one-dimensional, logarithmically spaced wave vectors $k_n = k_0 2^n$, $k_0 = 1/16$, complex conjugation is denoted by $*$, and the coefficients $a_n = k_n$, $b_n = -\delta k_{n-1}$, and $c_n = -(1 - \delta) k_{n-2}$, with $\delta = 1/2$, are chosen to conserve the shell-model analogs of energy and helicity in the inviscid, unforced limit. By construction, the velocity in a given shell is affected directly only by velocities in nearest- and next-nearest-neighbor shells. By contrast, all Fourier modes of the velocity field interact with each other in the Navier-Stokes equation as can be seen easily by writing it in wave-vector space. Thus, the GOY shell model does not have the sweeping effect by which modes (eddies) corresponding to the largest length scales affect all those at smaller length scales directly. Hence, it has been suggested that the GOY shell model should be thought of as a model for quasi-Lagrangian velocities [13]. We might anticipate therefore that GOY-model structure functions should not have the trivial dynamic scaling associated with Eulerian velocities; we show this explicitly below. We integrate the GOY model (9) by using the slaved, Adams-Bashforth scheme [14,15], and 22 shells ($1 \le n \le 22$), with $f_n = \delta_{n,1}(1 + i) \times 5 \times 10^{-3}$ (Table I). The equal-time structure function of order p and the associated exponent is defined by $S_p(k_n) = \langle |u_n|^p \rangle \sim k_n^{-\zeta_p}$. However, the static solution of Eq. (9) exhibits a three-cycle with the shell index n, which is effectively filtered out [12] if we use $\Sigma_p(k_n) \equiv \langle |\Im[u_{n+2} u_{n+1} u_n - (1/4) u_{n-1} u_n u_{n+1}]|^{p/3} \rangle \sim k_n^{-\zeta_p}$, to determine ζ_p. These exponents, shown in Table II, are in close agreement with those found for homogeneous, isotropic fluid turbulence in three dimensions [12]. We analyze the velocity $[u_n(t)]$ time series for $n = 4$ to 13, i.e., for wave vectors well within the inertial range [16].

For the GOY shell model we use the normalized, order-p, complex, time-dependent structure function

TABLE I. The viscosity ν, time step δt, Taylor microscale $\lambda \equiv (\sum_n |u_n|^2/k_n/\sum_n k_n|u_n|^2)^{1/2}$, the root-mean-square velocity $u_{\rm rms} \equiv [2\sum_n |u_n|^2/k_n/(2\pi k_1)]^{1/2}$, the Taylor-microscale Reynolds number $\mathrm{Re}_\lambda \equiv \lambda u_{\rm rms}/\nu$, the integral scale $L_{\rm int} \equiv (\sum_n |u_n|^2/k_n^2)/(\sum_n |u_n|^2/k_n)$, and the box-size eddy turnover time $\tau_L \equiv L_{\rm int}/u_{\rm rms}$ that we use in our numerical simulation of the GOY shell model. Data from the first $T_{\rm tr}$ time steps are discarded so that transients can die down. We then average our data for a time $T_{\rm av}$.

ν	δt	λ	$u_{\rm rms}$	Re_λ	$L_{\rm int}$	τ_L	$T_{\rm tr}$	$T_{\rm av}$
10^{-7}	2×10^{-4}	0.7	0.35	2×10^6	6.3	$10^5 \delta t$	$5 \times 10^4 \tau_L$	$10^5 \tau_L$

$f_p(n,t) \equiv \langle [u_n(0)u_n^*(t)]^{p/2} \rangle / S_p(k_n)$. The representative plot of Fig. 1 shows that the imaginary part of $f_p(n,t)$ is negligibly small compared to its real part. Hence, we work with the real part of $f_p(n,t)$, i.e., $F_p(n,t) \equiv \Re[f_p(n,t)]$.

Integral and derivative-time scales can be defined for the shell model (9) as in Eqs. (4) and (6). We now concentrate on the integral-time scale with $M = 1$, $T^I_{p,1}(n,t_u) \equiv \int_0^{t_u} F_p(n,t)dt$, the derivative-time scale with $M = 2$, $T^D_{p,2} \equiv [\partial^2 F_p(n,t)/\partial t^2|_{t=0}]^{-1/2}$, and the associated dynamic-multiscaling exponents defined via $T^I_{p,1}(n,t_u) \sim k_n^{-z^I_{p,1}}$ and $T^D_{p,2}(n) \sim k_n^{-z^D_{p,2}}$ [17]. The slope of a log-log plot of $T^I_{p,1}(n)$ versus k_n now yields $z^I_{p,1}$ (Fig. 1 and Table II). Preliminary data for $z^I_{p,1}$ were reported by us in Ref. [9]. For extracting the derivative scale $T^D_{p,2}$ we extend $F_p(n,t)$ to negative t via $F_p(n,-t) = F_p(n,t)$ and use a centered, sixth-order, finite-difference scheme to find $(\partial^2/\partial t^2)F_p(n,t)|_{t=0}$. A log-log plot of $T^D_{p,2}(n)$ versus k_n now yields the exponent $z^D_{p,2}$ (Fig. 1 and Table II).

In Ref. [13] dynamic-multiscaling exponents were extracted not from time-dependent structure functions but by using the following exit-time algorithm: Define the decorrelation time for shell n, at time t_i, to be $T_i(n)$, such that, $|u_n(t_i)||u_n(t_i + T_i)| \geq \lambda^{\pm 1}|u_n(t_i)|^2$, with $0 < \lambda < 1$. The order-p, degree-M exit-time scale for the shell n is

$$T^E_{p,M} \equiv \lim_{N\to\infty} \left[\frac{\frac{1}{N}\sum_{i=1}^N T_i^M |u_n(t_i)|^p}{\frac{1}{N}\sum_{i=1}^N |u_n(t_i)|^p} \right]^{(1/M)} \sim k_n^{-z^E_{p,M}}, \quad (10)$$

where the last proportionality follows from the dynamic-multiscaling ansatz. In practice we cannot take the limit $N \to \infty$; in a typical run of length $T_{\rm av}$ (Table I) $N \simeq 10^9$. By suitably adapting the multifractal formalism used above, we get the exit-time bridge relation $z^E_{p,M} = 1 + [\zeta_{p-M} - \zeta_p]/M$, obtained in Ref. [13] only for $M = 1$. Dynamic-multiscaling exponents obtained via this exit-time method are shown for $M = 1$ and $M = -2$ in Table II. The exit-time bridge relations for $M > 0$ are the analogs of the integral-time bridge relation (5) and those for $M < 0$ are the analogs of the derivative-time bridge relation (7). Our results do not depend on λ for $0.3 < \lambda < 0.8$.

Our numerical results for the equal-time exponents ζ_p (column 2), the dynamic exponents $z^I_{p,1}$ (columns 3 and 4), $z^D_{p,2}$ (columns 6 and 7), and $z^E_{p,1}$ and $z^E_{p,-2}$ (columns 5 and 8, respectively) for $1 \leq p \leq 6$ are given in Table II. The agreement of the exponents in columns 3 and 4 shows that the bridge relation (5) is satisfied (within error bars); a comparison of columns 6 and 7 shows that the bridge relation (7) is satisfied. By comparing columns 4 and 5 we see that the integral-time exponent $z^I_{p,1}$ is the same as the exit-time exponent $z^E_{p,1}$; columns 7 and 8 show that the derivative-time exponent $z^D_{p,2}$ is the same as the exit-time exponent $z^E_{p,-2}$. The relation $z^D_{2,1} = \zeta_2$ mentioned above [5] is not meaningful in the GOY model since $\partial F_p(n,t)/\partial t|_{t=0}$ vanishes (at the level of our numerical study). We have obtained 50 different values of each of the dynamic-multiscaling exponents from 50 different initial conditions. For each initial condition time averaging is done over a time $T_{\rm av}$ (Table I), which is larger than the averaging time of Ref. [13] by a factor of about 10^4. The means of these 50 values for each of the

TABLE II. Order-p (column 1) multiscaling exponents for $1 \leq p \leq 6$ from our simulations of the GOY model: equal-time exponents ζ_p (column 2), integral-scale dynamic-multiscaling exponent $z^I_{p,1}$ of degree 1 (column 3) from the bridge relation (5) and the values of ζ_p in column 1, $z^I_{p,1}$ from our calculation using time-dependent structure functions (column 4), the exit-time exponents of order 1 $z^E_{p,1}$ (column 5), the derivative-time exponents $z^D_{p,2}$ (column 6) from the bridge relation (7) and the values of ζ_p in column 1, $z^D_{p,2}$ from our calculation using time-dependent structure function (column 7), and the exit-time exponent of order -2, $z^E_{p,-2}$ (column 8). The error estimates are obtained as described in the text.

Order (p)	ζ_p	$z^I_{p,1}$ [Eq. (5)]	$z^I_{p,1}$	$z^E_{p,1}$	$z^D_{p,2}$ [Eq. (7)]	$z^D_{p,2}$	$z^E_{p,-2}$
1	0.3777 ± 0.0001	0.6221 ± 0.0001	0.60 ± 0.02	0.603 ± 0.007	0.6820 ± 0.0001	0.70 ± 0.02	0.677 ± 0.001
2	0.7091 ± 0.0001	0.6686 ± 0.0002	0.67 ± 0.02	0.661 ± 0.007	0.7081 ± 0.0002	0.71 ± 0.01	0.719 ± 0.004
3	1.0059 ± 0.0001	0.7030 ± 0.0002	0.701 ± 0.009	0.708 ± 0.001	0.7310 ± 0.0002	0.73 ± 0.01	0.739 ± 0.006
4	1.2762 ± 0.0002	0.7298 ± 0.0003	0.727 ± 0.007	0.74 ± 0.01	0.7509 ± 0.0003	0.744 ± 0.009	0.758 ± 0.006
5	1.5254 ± 0.0005	0.7511 ± 0.0007	0.759 ± 0.009	0.77 ± 0.01	0.7684 ± 0.0007	0.756 ± 0.009	0.778 ± 0.003
6	1.757 ± 0.001	0.768 ± 0.002	0.77 ± 0.01	0.79 ± 0.01	0.7836 ± 0.002	0.764 ± 0.009	0.797 ± 0.0008

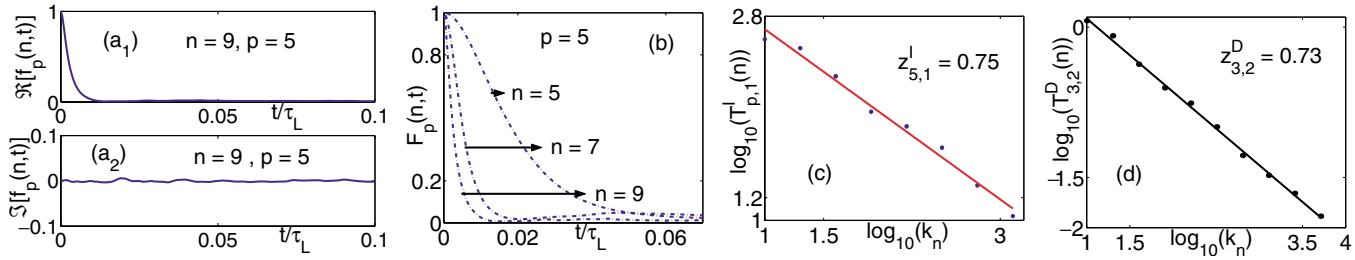

FIG. 1 (color online). Plots of real (a_1) and imaginary (a_2) parts of the time-dependent structure function $f_p(n, t)$ for the GOY shell model for shell number $n = 9$ and order $p = 5$ versus time t/τ_L, where τ_L is the box-size eddy turnover time (Table I). Note that $\Im[f_p(n, t)]$ is negligibly small compared to $F_p(n, t) = \Re[f_p(n, t)]$. (b) $F_p(n, t)$ versus t/τ_L for $p = 5$ and $n = 5$, 7, and 9. Representative log-log plots (base 10) of the integral (c) and derivative (d) time scales $T^I_{5,1}(n)$ and $T^D_{3,2}(n)$ versus k_n; the slopes of the linear least-square fits in (c) and (d) yield the dynamic exponents $z^I_{5,1}$ and $z^D_{3,2}$, respectively.

dynamic-multiscaling exponents are shown in Table II; the standard deviation yields the error. This averaging is another way of removing the effects of the three-cycle mentioned before.

We have shown systematically how different ways of extracting time scales from time-dependent velocity structure functions or time series can lead to different sets of dynamic-multiscaling exponents, which are related in turn to the equal-time multiscaling exponents ζ_p by different classes of bridge relations. Our extensive numerical study of the GOY shell model for fluid turbulence verifies explicitly that such bridge relations hold. Experimental studies of Lagrangian quantities in turbulence have been increasing [18]. We hope our work will stimulate studies of dynamic multiscaling in such experiments. Furthermore, the sorts of bridge relations we have discussed here must also hold in other problems, with multiscaling of equal-time and time-dependent structure functions or correlation functions, such as passive-scalar and magnetohydrodynamic turbulence. As we will report elsewhere [19] the intermittency of the advecting velocity field is *crucial* for dynamic multiscaling in the passive-scalar case. For the Kraichnan model, in which the passive scalar is advected by a zero-mean, Gaussian velocity field that is white in time and whose variance scales as ℓ^ξ, $z^D_{p,1} = z^I_{p,M} = 2 - \xi$ for all p and M, even though passive-scalar, equal-time structure functions exhibit multiscaling; if the advecting velocity field is intermittent, then dynamic multiscaling is obtained. Numerical studies of time-dependent, quasi-Lagrangian-velocity structure functions in the Navier-Stokes equation, already under way, will also be discussed elsewhere.

We thank A. Celani, S. K. Dhar, U. Frisch, S. Ramaswamy, A. Sain, and especially C. Jayaprakash for discussions, the IFCPAR (Project No. 2404-2), and CSIR (India) for support.

*Also at Jawaharlal Nehru Centre for Advanced Scientific Research, Jakkur, Bangalore, India.

[1] P. C. Hohenberg and B. I. Halperin, Rev. Mod. Phys. **49**, 435 (1977), and references therein.
[2] U. Frisch, *Turbulence: The Legacy of A. N. Kolmogorov* (Cambridge University, Cambridge, England, 1996).
[3] V. S. L'vov, E. Podivilov, and I. Procaccia, Phys. Rev. E **55**, 7030 (1997).
[4] F. Hayot and C. Jayaprakash, Phys. Rev. E **57**, R4867 (1998).
[5] F. Hayot and C. Jayaprakash, Int. J. Mod. Phys. B **14**, 1781 (2000).
[6] A. N. Kolmogorov, Dokl. Akad. Nauk SSSR **30**, 9 (1941) [, C. R. Acad. Sci. URSS **30**, 301 (1941)].
[7] V. I. Belinicher and V. S. L'vov, Sov. Phys. JETP **66**, 303 (1987).
[8] Y. Kaneda, T. Ishihara, and K. Gotoh, Phys. Fluids **11**, 2154 (1999).
[9] D. Mitra and R. Pandit, Physica (Amsterdam) **318A**, 179 (2003).
[10] In Ref. [4] case (b) appears as a subdominant contribution to the dominant sweeping contribution.
[11] E. B. Gledzer, Sov. Phys. Dokl. **18**, 216 (1973); K. Ohkitani and M. Yamada, Prog. Theor. Phys. **81**, 329 (1989).
[12] L. P. Kadanoff, D. Lohse, J. Wang, and R. Benzi, Phys. Fluids **7**, 617 (1995).
[13] L. Biferale, G. Bofetta, A. Celani, and F. Toschi, Physica (Amsterdam) **127D**, 187 (1999).
[14] S. K. Dhar, A. Sain, and R. Pandit, Phys. Rev. Lett. **78**, 2964 (1997).
[15] D. Pisarenko, L. Biferale, D. Courvoisier, U. Frisch, and M. Vergassola, Phys. Fluids A **5**, 2533 (1993).
[16] The smaller the wave vector k_n, the slower is the evolution of $u_n(t)$, so we use different temporal sampling rates for velocities in different shells: $50 \times \delta t$ for $4 \leq n \leq 8$ and $10 \times \delta t$ for $9 \leq n \leq 13$, respectively.
[17] In principle, $t_u \to \infty$ but, since it is not possible to obtain $F_p(n, t)$ accurately for large t, we select an upper cutoff t_u such that $F_p(n, t_u) = \alpha$, where, for all n and p, we choose $\alpha = 0.7$ here. Our results do not change if $0.3 < \alpha < 0.8$.
[18] See, e.g., S. Ott and J. Mann, J. Fluid Mech. **422**, 207 (2000); A. La Porta, G. A. Voth, A. M. Crawford, J. Alexander, and E. Bodenschatz, Nature (London) **409**, 1017 (2002); N. Mordant, P. Metz, O. Michel, and J.-F. Pinton, Phys. Rev. Lett. **87**, 214501 (2001).
[19] D. Mitra and R. Pandit (to be published).